Desalination and Water Treatment
www.deswater.com
doi: 10.1080/19443994.2013.852482

53 (2015) 1335–1341
February

Taylor & Francis
Taylor & Francis Group

The effect of operational parameters in the photocatalytic activity of synthesized Mg/ZnO–SnO_2 nanoparticles

Mohammad A. Behnajady*, Yasamin Tohidi

Faculty of Science, Department of Chemistry, Tabriz Branch, Islamic Azad University, Tabriz, Iran
Email: behnajady@iaut.ac.ir

Received 20 January 2013; Accepted 1 October 2013

ABSTRACT

In this study, ZnO–SnO_2 nanoparticles were prepared using the co-precipitation method, and then to reach higher photocatalytic activity, Mg was impregnated onto the prepared nanoparticles. The results of BET analysis indicated that compared to pure ZnO–SnO_2, Mg/ZnO–SnO_2 nanoparticles had a higher specific surface area. The photocatalytic performance of synthesized samples was monitored by degradation rate of Methyl Orange (MO) as a probe pollutant under UV light irradiation. In order to get more information for optimization of photocatalytic activity, the effect of various operational parameters (i.e. catalyst dosage, MO concentration, pH, and light intensity) were investigated. The results revealed that the highest removal percentage of MO was achieved with 800 mg L^{-1} of Mg/ZnO–SnO_2, 10 mg L^{-1} of MO at pH = 4.5, and light intensity of 62.2 W m^{-2}. The synthesized samples demonstrated superior photocatalytic activity than TiO_2–P25 nanoparticles.

Keywords: ZnO–SnO_2; Mg impregnation; Photocatalytic activity; Methyl Orange

1. Introduction

Heterogeneous photocatalysis by using semiconductors (e.g. TiO_2, ZnO, etc.) under UV light illumination has recently gained enormous attention due to high potential in complete removal of organic contaminants [1]. Upon being irradiated with energy greater than the band gap energy of semiconductors, electrons are excited to the conduction band, leaving holes in the valance band. Afterwards, the formation of highly reactive species, such as hydroxyl radicals (as a result of holes reaction with surface hydroxide ions or H_2O molecules) leads to the decomposition of toxic pollutants into practically innocuous products such as CO_2 and H_2O [2,3]. Unfortunately, the rapid recombination rate of electron-hole pairs diminishes the efficiency of photocatalysis, thus restricting its application in industrial sector. Therefore, lowering the recombination of charge carriers is of great importance and has attained extensive attention in recent years [4]. Semiconductor/semiconductor and/or metal/semiconductor heterostructures can be an effective approach to achieve this goal [5]. In the case of semiconductor/semiconductor heterostructures (i.e. ZnO–SnO_2, ZnO–TiO_2, SnO_2–TiO_2), due to redox energy level differences between conduction and valance bands of different semiconductors, the electrons are transferred from the photoactivated semiconductor to the non-photoactivated semiconductor, and holes are transferred in the opposite direction. Thus, the recombination rate of the photoinduced electron-hole pairs will decrease, leading to higher photocatalytic activity than the semiconductors used alone [6–11]. As for the

*Corresponding author.

metal/semiconductor heterostructures, it is deduced that incorporated dopants can act as a trap for charge carriers. Therefore, the lifetime of electron-hole pairs and consequently hydroxyl radical formation will increase [12]. Likewise, doping may increase the specific surface area of the semiconductor and improve pollutant adsorption on the catalyst, resulting in an improved photocatalytic activity [13]. Different metals including Mg have been used to increase the photocatalytic activity in various studies. Mg^{2+}-doped TiO_2 exhibited a better photocatalytic activity than pure nano TiO_2 and commercial TiO_2–P25 for degradation of 4-chlorophenol (4-CP). The enhanced adsorption of 4-CP over catalyst surface and decrease in particle size were believed to be the reason for higher photocatalytic activity [14]. Similarly, Feng et al. [15] observed that among different doped TiO_2 catalysts, Mg-doped TiO_2 had the highest photocatalytic activity in the removal of Rhodamine B. This was due to the dye sensitization mechanism which occurred during the degradation process. A better photocatalytic activity of Mg-doped semiconductors in comparison with pure semiconductors was observed by Behnajady et al. and Ileperuma et al. as well [16,17]. In order to investigate further photocatalytic improvement by considering the possible advantages of combining both coupling and impregnation methods, in this study synthesized Mg/ZnO–SnO_2 nanophotocatalyst was used to remove Methyl Orange (MO) from aqueous solution. The effect of different operational parameters was also studied. TiO_2–P25 was used as a reference photocatalyst to evaluate Mg/ZnO–SnO_2 photocatalytic efficiency.

2. Experiment

2.1. Preparation of nanophotocatalysts

To prepare Mg/ZnO–SnO_2 nanophotocatalyst, ZnO–SnO_2 nanoparticles were synthesized according to the procedure described in the literature [7]. For impregnation with Mg to 1 g of ZnO–SnO_2 precursor in 30 mL deionized water, 0.8 mol% $Mg(NO_3)_2{\cdot}6H_2O$ (Scharlau) was added. The resulting suspension was ultrasonically dispersed for 15 min and later subjected to reflux at 80°C for 4 h. The resulting precipitates, after being cooled down to the room temperature, were filtered and washed with deionized water several times. The precipitates were dried at 80°C for 10 h and finally calcined at 350°C for 1 h. The synthesized samples were characterized by XRD (Siemens D5000 diffractometer), FESEM (Hitachi S4160), EDX (Vegal Tescan), BET (Belsorp mini II), and TEM (Philips CM10) methods.

2.2. Photocatalytic activity measurements

After adjusting the pH value at the desired level, reaction suspensions (100 mL) containing a specified amount of Mg/ZnO–SnO_2 nanophotocatalyst and MO were kept in darkness for 30 min. Oxygen was bubbled in order to reach adsorption–desorption equilibrium. The reaction was initiated when UV lamp (15 W, UV-C, λ_{max} = 254 nm, manufactured by Philips) was switched on. Samples were taken out at specific time intervals and centrifuged at 1,000 rpm. The remaining concentration of MO in solution was analyzed by UV–vis spectrophotometer (Pharmacia Biotech, Ultrospec 2000) at its maximum wavelength of 465 nm.

3. Results and discussion

3.1. Crystallite structure and morphology of synthesized samples

XRD technique was used to characterize the crystallite structure of Mg/ZnO–SnO_2 nanoparticles calcined at 350°C. As it is shown in Fig. 1, all the observed diffraction peaks are indexed to ZnO and SnO_2 without any impurity peak relating to Mg, which can be due to low Mg concentration [16]. The crystallite size of the synthesized nanoparticles was estimated by using the Scherrer formula. The diffraction peaks related to SnO_2 were broad, revealing a small mean crystallite size, which was estimated to be about 4.2 nm, while the diffraction peaks related to ZnO were rather sharp with an average crystallite size of about 15.9 nm. It has been reported that the presence of SnO_2 causes an increase in the crystallite size

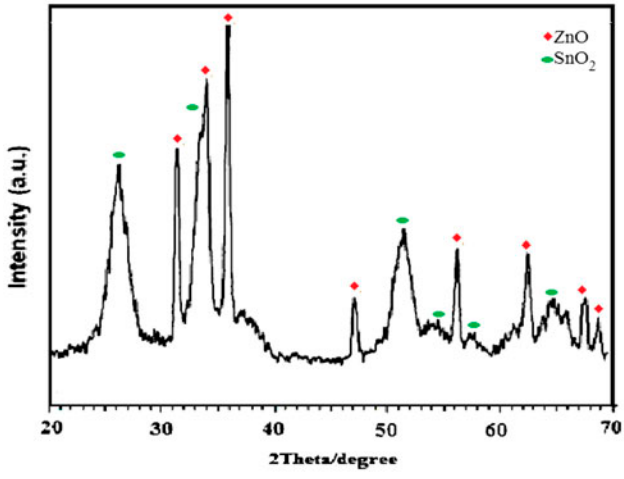

Fig. 1. XRD pattern of Mg/ZnO–SnO_2 nanoparticles calcined at 350°C.

of ZnO, whereas the presence of ZnO restrains the growth of SnO_2 nanocrystals [11].

The morphology of Mg/ZnO–SnO_2 nanoparticles was investigated by FESEM micrograph. The typical FESEM image (Fig. 2) demonstrates that the synthesized samples are nanosized and spherical in shape. The uniform dispersion of synthesized nanoparticles is obvious as well.

EDX analysis revealed that the Zn, Sn, and Mg amount in Mg/ZnO–SnO_2 nanoparticles were about 58.35, 31.21, and 2.26 wt.%, respectively. The analytical results from EDX indicated that much more Mg elements had been impregnated onto ZnO–SnO_2 nanoparticles. The specific surface area of synthesized samples determined by BET method was calculated to be 32.051 and 49.065 $m^2\ g^{-1}$ for ZnO–SnO_2 and Mg/ZnO–SnO_2 nanoparticles, respectively. As a consequence, Mg impregnation leads to higher specific surface area and thus higher photocatalytic activity in comparison with pure ZnO–SnO_2 nanoparticles. In order to gain better information about the morphology of Mg/ZnO–SnO_2 nanoparticles, TEM technique was used. As it is seen in Fig. 3, the synthesized samples are nanosized and uniformly dispersed. The spherical shape of these nanoparticles is apparent as well.

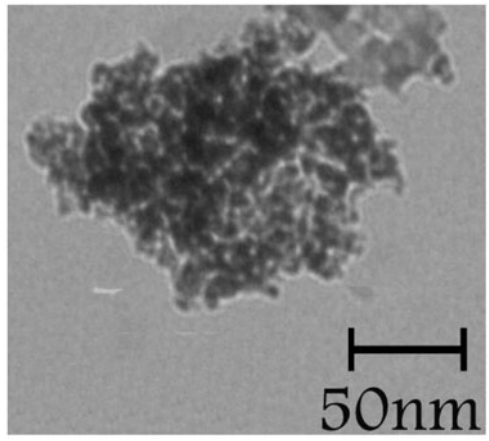

Fig. 3. TEM micrograph of Mg/ZnO–SnO_2 nanoparticles.

3.2. Photocatalytic activity

3.2.1. The preliminary tests

The photocatalytic removal of MO in the solution was studied in the presence of pure ZnO–SnO_2 and Mg/ZnO–SnO_2 photocatalysts. A blank sample (without any catalyst) was also irradiated under the same condition. The obtained results revealed that the removal of MO was insignificant when no catalyst was used, while impregnation with Mg greatly improved the photocatalytic activity of pure ZnO–SnO_2. Accordingly, the removal efficiency of MO, after 40 min of UV irradiation time, was 19.9% without catalyst, 70.4 and 83.7% for pure ZnO–SnO_2 and Mg/ZnO–SnO_2, respectively.

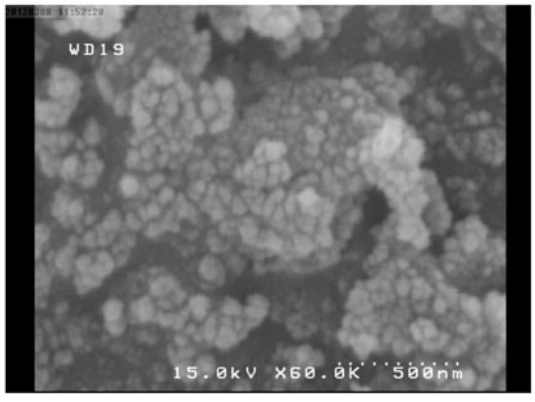

Fig. 2. FESEM image of Mg/ZnO–SnO_2 nanoparticles.

3.2.2. The effect of catalyst dosage

Mg/ZnO–SnO_2 in the range of 200–900 mg L^{-1} was selected to investigate the removal rate of MO from aqueous solution. Results in Fig. 4 indicated that the apparent first-order rate constant (k_{ap}) enhanced by increasing catalyst dosage up to 800 mg L^{-1}, but further increase up to 900 mg L^{-1} had no significant effect on photocatalytic efficiency. The more catalyst

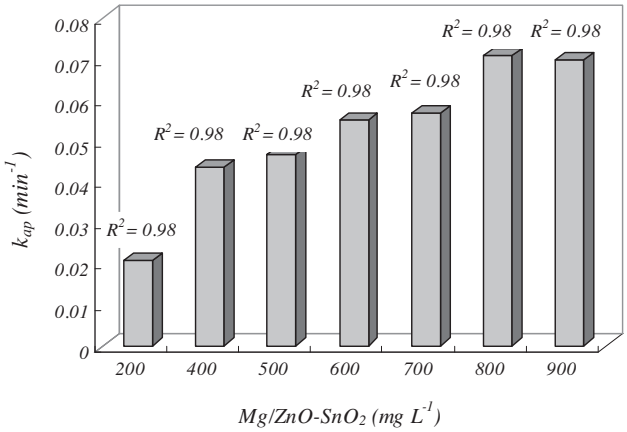

Fig. 4. The effect of catalyst dosage on photocatalytic activity of Mg/ZnO–SnO_2 nanophotocatalyst (I_0 = 62.2 W m^{-2}, [MO] = 10 mg L^{-1}).

dosage is, the more number of active sites on the catalyst surface will be. Thus, the formation of hydroxyl radicals and adsorption of MO molecules on catalyst surface increase and consequently photocatalytic performance will be enhanced [2]. On the other hand, when the catalyst dosage rises above a desired level, the amount of UV light reaching the surface of photocatalyst is reduced. As a result, the formation of hydroxyl radicals, the number of active sites on catalyst surface, and surface area available for photon absorption diminish leading to lower photocatalytic activity [18,19]. A number of different studies have shown that the photocatalytic degradation of different pollutants initially increases with increase in catalyst dosage and then decreases when the catalyst dosage reaches above the optimal value. This phenomenon has been explained by light scattering, reduction of surface area, etc. [19]. Behnajady et al. [20] reported an optimum catalyst loading of 200 mg L^{-1} for silver doped TiO_2 for the degradation of C.I. Acid Red 88 (AR88). But when the catalyst dosage was raised above the limiting value, the UV light penetration due to an increase in the turbidity of solution increased, resulting in decreased AR88 degradation.

3.2.3. Effect of MO concentration

In order to study the effect of MO concentration, a series of tests were conducted with 800 mg L^{-1} Mg/ZnO–SnO_2 and MO concentration of 5–30 mg L^{-1} (Fig. 5). It is clear that the removal efficiency of MO is in close relationship with the probability of hydroxyl radical formation at catalyst surface. As the concentration of MO increases, the photons get intercepted before they can reach the catalyst surface, and consequently formation of electron-hole pairs and photocatalytic efficiency is reduced [6,21]. For higher MO concentration, more reactive species ($OH^{\bullet}$, $O_2^{-\bullet}$) are needed, but at a fixed catalyst amount, light intensity and irradiation time, the formation of $OH^{\bullet}$ and $O_2^{-\bullet}$ will be kept at a fixed level; thus, the efficiency of MO removal will be reduced [19]. Wu et al. [22] observed that by increasing initial dye concentration from 20 to 40 mg L^{-1}, the decolorization rate constant decreased. The decreased photocatalytic activity was attributed to constant hydroxyl radical formation on the surface of catalyst. Therefore, the number of hydroxyl radicals attacking dye molecules declined. Similar results were reported for the degradation of Methylene Blue in the range of 5–10 mg L^{-1} by Talebian et al. [23].

3.2.4. Effect of pH

It is known that dye removal is greatly influenced by the pH of solution. ZnO is an amphoteric oxide which is stable at $4 \le pH \le 14$; otherwise, it will be dissolved [24]. Since the transition pH range for MO stays at 3.1–4.4, the experiments were conducted at pH = 4.54, 7.46, and 9.52 with 800 mg L^{-1} Mg/ZnO–SnO_2 and 10 mg $L^{-1}$of MO. The obtained results are depicted in Fig. 6. As it is seen, the removal of MO is favored at pH = 4.5. It is worth noting that the pH values adopted in this work are greater than pK_a value (3.47) for MO; thus, MO will be in its anionic form in the solution. The zero point charge pH (pH_{zpc}) for ZnO and SnO_2 is considered to be 9.0 ± 0.3 and ~ 5.5, respectively. At pH higher than pH_{zpc}, the surface of ZnO and SnO_2 will be negatively

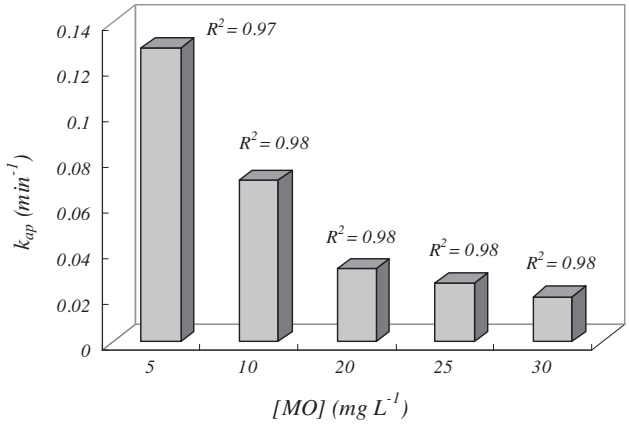

Fig. 5. The effect of MO concentration on photocatalytic activity of Mg/ZnO–SnO_2 nanophotocatalyst (I_0 = 62.2 W m^{-2}, [Mg/ZnO–SnO_2] = 800 mg L^{-1}).

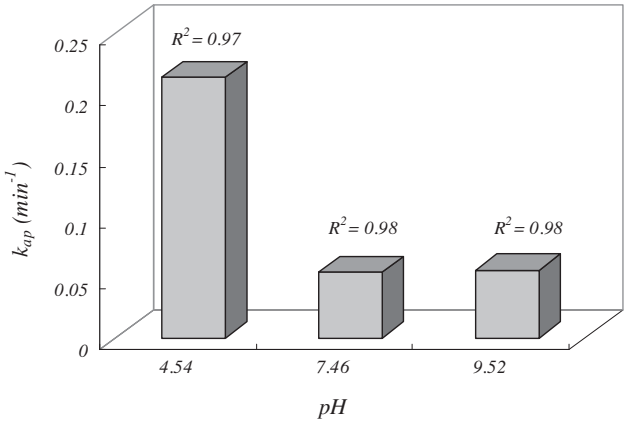

Fig. 6. The effect of pH on photocatalytic activity of Mg/ZnO–SnO_2 nanophotocatalyst (I_0 = 62.2 W m^{-2}, [MO] = 10 mg L^{-1}, [Mg/ZnO–SnO_2] = 800 mg L^{-1}).

charged while at pH < pH_{zpc} their surfaces will be charged positively [25,26].

At lower pH values, there will be a strong interaction among MO anions and positively charged catalyst surface. As the pH value increases, the electrostatic repulsion among MO anions and negatively charged catalyst surface increases; consequently, the MO adsorption on the catalyst and degradation efficiency decreases. The same results were observed by Zhiyong et al. while investigating the removal of Orange Π as a function of pH. The removal was favored at lower pH values (i.e. pH 3.0 and 5.9) but was slower at higher pH value (i.e. pH 10) [27].

3.2.5. Effect of light intensity

UV light is a key factor in heterogeneous photocatalysis, since it provides the photons required for electron-hole formation. To study the effect of this parameter by keeping other parameters at their desired level, the UV light intensity was varied from 31 to 62.2 W m^{-2} by changing the distance between UV lamp and photoreactor.

The results (Fig. 7) indicated that the highest dye removal was obtained with light intensity of 62.2 W m^{-2}. The number of photons absorbed by the catalyst enhances with increasing the light intensity. With the increase of the number of absorbed photons, the formation of electron-hole pairs and hydroxyl radicals will also increase, and thus, the efficiency of photocatalysis will be improved [21]. On the other hand, the competition among formation and recombination of electron-hole pairs at lower intensities would decrease the photocatalytic efficiency [16]. Some researchers have noted the same results while studying the effect of UV light intensity on the degradation of dyes [6,19]. The increased value of k_{ap} by increasing UV light intensity is associated with higher hydroxyl radical formation by Behnajady et al. for degradation of AR88 [21].

3.2.6. Comparison of photocatalytic activity with TiO_2–P25 and spectral changes of MO

In order to get a better insight into Mg/ZnO–SnO_2 photocatalytic efficiency, its activity was compared with TiO_2–P25 as a reference catalyst (Fig. 8). In this case, the k_{ap} was reported per surface area (min^{-1} m^{-2}) in order to have more explicit and comparable data. At the desired operational conditions, Mg/ZnO–SnO_2 nanophotocatalyst exhibited better activity than TiO_2–P25 nanoparticles. It seems that coupling two semiconductor oxides with different band gap widths and also impregnation with Mg lead to a higher photocatalytic activity than TiO_2–P25 nanoparticles under the same conditions.

The photocatalytic performance of Mg/ZnO–SnO_2 in the degradation of MO was evaluated by diminishing of MO peaks in the UV and visible regions. As depicted in Fig. 9, two major peaks around 225 and 465 nm are associated with MO absorption spectrum. The one at 225 nm is attributed to aromatic rings and the latter to –N=N– chromophore structure. Upon UV light illumination, both peaks gradually vanish and MO is completely removed after 40 min. The observed diminishing trend at 225 and 465 nm accounts for mineralization of aromatic rings and decomposition of chromophore structure, respectively.

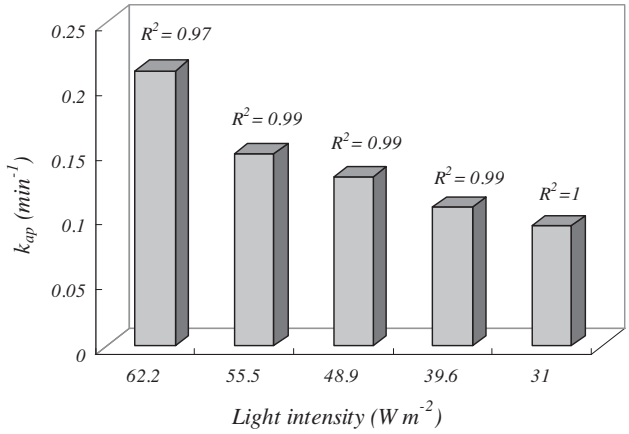

Fig. 7. The effect of light intensity on photocatalytic activity of Mg/ZnO–SnO_2 nanophotocatalyst (pH = 4.5, [MO] = 10 mg L^{-1}, [Mg/ZnO–SnO_2] = 800 mg L^{-1}).

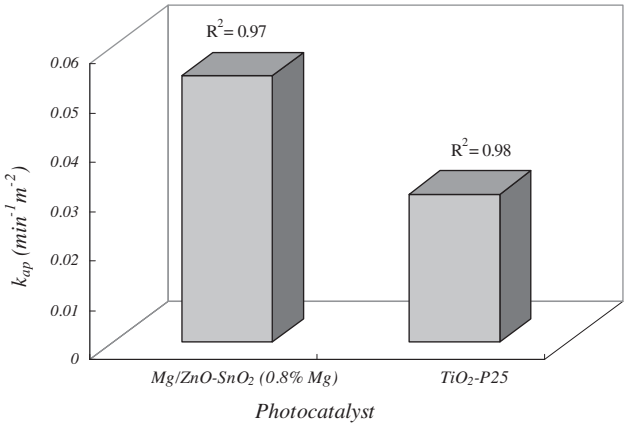

Fig. 8. Comparison of photocatalytic efficiency of Mg/ZnO–SnO_2 and TiO_2–P25 (I_0 = 62.2 W m^{-2}, [MO] = 10 mg L^{-1}, pH = 4.5).

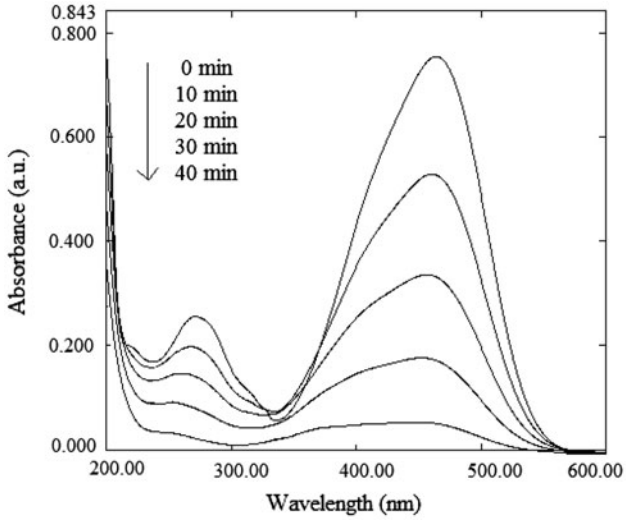

Fig. 9. Absorption spectrum of MO at different irradiation times ([Mg/ZnO–SnO_2] = 400 mg L^{-1}, [MO] = 10 mg L^{-1}, I_0 = 62.2 W m^{-2}).

4. Conclusion

In this study, Mg/ZnO–SnO_2 nanophotocatalyst with 0.8 mol % Mg was successfully synthesized. The prepared samples exhibited a high photocatalytic activity for MO removal, and then its photocatalytic activity was compared with TiO_2–P25 as a reference catalyst. The synthesized samples showed superior photocatalytic activity than TiO_2–P25 nanoparticles. Also, the effect of different operational parameters (i.e. catalyst dosage, MO concentration, pH, and UV light intensity on photocatalytic activity) was studied. The results indicated that by setting operational parameters at their desired level, the photocatalytic activity will further improve. The removal rate of MO was found to increase by increasing Mg/ZnO–SnO_2 dosage up to 800 mg L^{-1} for MO concentration of 10 mg L^{-1} in the acidic solution (i.e. pH = 4.5) and under UV light intensity of 62.2 W m^{-2}.

Acknowledgements

The authors thank the financial support of Tabriz Branch, Islamic Azad University and the Iranian Nanotechnology Initiative Council.

References

[1] R. Liu, Y. Huang, A. Xiao, H. Liu, Preparation and photocatalytic property of mesoporous ZnO/SnO_2 composite nanofibers, J. Alloys Compd. 503 (2010) 103–110.

[2] J. Nishio, M. Tokumura, H.T. Znad, Y. Kawase, Photocatalytic decolorization of azo-dye with zinc oxide powder in an external UV light irradiation slurry photoreactor, J. Hazard. Mater. B 138 (2006) 106–115.

[3] Z. Yang, L. Lv, Y. Dai, Z. Xv, D. Qian, Synthesis of ZnO/SnO_2 composite oxides by CTAB-assisted co-precipitation and photocatalytic properties, Appl. Surf. Sci. 256 (2010) 2898–2902.

[4] M. Zhang, T. An, X. Hu, C. Wang, G. Sheng, J. Fu, Preparation and photocatalytic properties of a nanometer ZnO–SnO_2 coupled oxide, Appl. Catal. A 260 (2004) 215–222.

[5] L. Zheng, Y. Zheng, C. Chen, Y. Zhan, X. Lin, Q. Zheng, K. Wei, J. Zhu, Network structured SnO_2/ZnO heterojunction nanocatalyst with high photocatalytic activity, Inorg. Chem. 48 (2009) 1819–1825.

[6] N. Modirshahla, A. Hassani, M.A. Behnajady, R. Rhbarfam, Effect of operational parameters on decolorization of acid yellow 23 from wastewater by UV irradiation using ZnO and ZnO/SnO_2 photocatalysts, Desalination 271 (2011) 187–192.

[7] C. Wang, X. Wang, B.Q. Xu, J. Zhao, B. Mai, P. Peng, G. Sheng, J. Fu, Enhanced photocatalytic performance of nanosized coupled ZnO/SnO_2 photocatalysts for methyl orange degradation, J. Photochem. Photobiol. A 168 (2004) 47–52.

[8] M. Zhang, G. Sheng, J. Fu, T. An, X. Wang, X. Hu, Novel preparation of nanosized ZnO–SnO_2 with high photocatalytic activity by homogeneous co-precipitation method, Mater. Lett. 59 (2005) 3641–3644.

[9] X. Jia, H. Fan, L. Qin, C. Yang, Hierarchically structure SnO_2/ZnO nanocomposites: Growth, mechanism and gas sensing property, J. Dispersion Sci. Technol. 31 (2010) 1405–1408.

[10] Z. Wang, Z. Li, H. Zhang, C. Wang, Improved photocatalytic activity of mesoporous ZnO/SnO_2 coupled nanofibers, Catal. Commun. 11 (2009) 257–260.

[11] Md. Tamez Uddin, Y. Nicolas, C. Olivier, T. Toupance, L. Servant, M.M. Muller, H.J. Kleebe, J. Ziegler, W. Jaegermann, Nanostructured SnO_2/ZnO heterojunction photocatalyst showing enhanced photocatalytic activity for degradation of organic dyes, Inorg. Chem., 51 (2012) 7764–7773.

[12] J.C. Colmenares, M.A. Aramendia, A. Marinas, J.M. Marinas, F.J. Urbano, Synthesis, characterization and photocatalytic activity of different metal-doped titania systems, Appl. Catal. A 306 (2006) 120–127.

[13] S. Ahmed, M.G. Rasul, R. Brown, M.A. Hashib, Influence of parameters on the heterogeneous photocatalytic degradation of pesticides and phenolic contaminants in wastewater: A short review, J. Environ. Manage. 92 (2011) 311–330.

[14] N. Venkatachalam, M. Palanichamy, V. Murugesan, Sol-gel preparation and characterization of alkaline earth metal doped nano TiO_2: Efficient photocatalytic degradation of 4-chlorophenol, J. Mol. Catal A: Chem. 273 (2007) 177–185.

[15] H. Feng, L.E. Yu, M.-H. Zhang, Ultrasonic synthesis and photocatalytic performance of metal-ions doped TiO_2 catalysts under solar light irradiation, Mater. Res. Bull. 48 (2013) 672–681.

[16] M.A. Behnajady, B. Alizade, N. Modirshahla, Synthesis of Mg-doped TiO_2 nanoparticles under different

conditions and its photocatalytic activity, Photochem. Photobiol. 87 (2011) 1308–1314.
[17] O.A. Ileperuma, K. Tennakone, W.D.D.P. Dissanayake, Photocatalytic behaviour of metal doped titanium dioxide: Studies on the photochemical synthesis of Ammonia on Mg/TiO_2 catalyst systems, Appl. Catal. 62 (1990) L1–L5.
[18] U.G. Akpan, B.H. Hameed, Parameters affecting the photocatalytic degradation of dyes using TiO_2-based photocatalysts: A review, J. Hazard. Mater. 170 (2009) 520–529.
[19] S. Ahmed, M.G. Rasul, W.N. Martens, R. Brown, M.A. Hashib, Advances in heterogeneous photocatalytic degradation of phenols and dyes in wastewater: A review, Water, Air, and Soil Pollut. 215 (2011) 3–29.
[20] M.A. Behnajady, N. Modirshahla, M. Shokri, B. Rad, Enhancement of photocatalytic activity of TiO_2 nanoparticles by silver doping: Photodeposition vs. liquid impregnation methods, Global Nest J. 10 (2008) 1–7.
[21] M.A. Behnajady, S. Ghorbanzadeh Moghaddam, N. Modirshahla, M. Shokri, Investigation of the effect of heat attachment method parameters at photocatalytic activity of immobilized ZnO nanoparticles on glass plate, Desalination 249 (2009) 1371–1376.
[22] C.H. Wu, C.L. Chang, Decolorization of Reactive Red 2 by advanced oxidation processes: Comparative studies of homogeneous and heterogeneous systems, J. Hazard. Mater. B 128 (2006) 265–272.
[23] N. Talebian, M.R. Nilforoushan, Comparative study of the structural, optical and photocatalytic properties of semiconductor metal oxides toward degradation of methylene blue, Thin Solid Films 518 (2010) 2210–2215.
[24] W. Cun, Z. Jincai, W. Xinming, M. Bixian, S. Guoying, P. Ping'an and F. Jiamo, Preparation, characterization and photocatalytic activity of nano-sized ZnO/SnO_2 coupled photocatalysts, Appl. Catal. B 39 (2002) 269–279.
[25] E.S. Elmolla, M. Chaudhuri, Degradation of amoxicillin, ampicillin and cloxacillin antibiotics in aqueous solution by the UV/ZnO photocatalytic process, J. Hazard. Mater 173 (2010) 445–449.
[26] M.L. Toebes, J.A. Van Dillen, K.P. De Jong, Synthesis of supported palladium catalysts, J. Mol. Catal. A: Chem., 173 (2001) 75–98.
[27] Y. Zhiyong, M. Bensimon, V. Sarria, I. Stolitchnov, W. Jardim, D. Laub, E. Mielczarski, J. Mielczarski, L. Kiwi-Minsker, J. Kiwi, $ZnSO_4$-TiO_2 doped catalyst with higher activity in photocatalytic processes, Appl. Catal. B 76 (2007) 185–195.